Desalination and Water Treatment
www.deswater.com

doi:10.5004/dwt.2017.20652

76 (2017) 83–97
May

Analysis of antifouling behavior of high dispersible hydrophilic poly (ethylene glycol)/vinyl functionalized SiO_2 nanoparticles embedded polyethylene membrane

Ali Akbari[a], Reza Yegani[a,*], Behzad Pourabbas[b], Ali Behboudi[a]

[a]*Faculty of Chemical Engineering, Membrane Technology Research Center, Sahand University of Technology, Tabriz, Iran, email: akbari.sut@gmail.com (A. Akbari), ryegani@sut.ac.ir (R. Yegani), behboudi.sut@gmail.com (A. Behboudi)*
[b]*Faculty of Polymer Engineering, Sahand University of Technology, Tabriz, Iran, email: pourabas@sut.ac.ir (B. Pourabbas)*

Received 21 September 2016; Accepted 3 March 2017

ABSTRACT

In this work, nanocompsite membranes containing high density polyethylene (HDPE) and functionalized SiO_2 nanoparticles were fabricated via thermally induced phase separation method. Silica nanoparticles were functionalized by grafting of poly(ethylene glycol) (PEG) and vinyl functional groups to improve both interfacial adhesion and hydrophilic characteristics of the nanoparticles. HDPE nanocomposite membranes were fabricated by incorporation of the functionalized particles into polymer matrix in the presence of dicumyl peroxide as a free radical initiator. EDAX and BSE analyses showed that a high dispersion of nanoparticles could be achieved in the presence of vinyl moieties due to significant improvement in interaction between particles and HDPE chains. FE-SEM images showed that the vinyl grafted particles embedded membranes has an interconnected structure with interwoven polyethylene fibers. It was seen that pure water flux increases from 11 $L \cdot m^{-2} h^{-1}$ to higher than 90 $L \cdot m^{-2} h^{-1}$ in the presence of 2 wt.% PEG/vinyl grafted nanoparticles, compared to pure HDPE membrane. The obtained results confirmed that incorporation of PEG/vinyl grafted nanoparticles, caused to achieve a fouling resistance membrane during filtration of humic acid solution, even at higher loading of nanoparticles. Also, pre-treatment with polyaluminium chloride could significantly mitigate fouling and improve humic acid removal. It means that by using the polyethylene microfiltration membrane combined with coagulation process,the results were obtained similar to UF membranes, which usually require higher operation pressure and severe fouling drawbacks.

Keywords: HDPE nanocomposite membrane; Antifouling behavior; Hydrophilicity; Dispersibility; Functionalized SiO_2 nanoparticles

1. Introduction

As a green technology, membrane based separations play an important role in many industrial applications, like water and waste water treatment, food processing, pharmaceutical industry, and gas purification. The advantages of membrane technology over conventional separation methods make the membranes more demandable [1].

Fabrication of highly permeable, long standing, less fouling and economical membranes is essential for the sustainable growth of membrane dependent industries. By far most of the commercial membranes are made from organic polymers. Among the polymers, polyolefins such as polypropylene (PP) and polyethylene (PE) are good candidates for preparing cheap, thermally stable and chemically resistant membranes [2,3].

Generally, due to the lack of solvents at low temperatures, thermally induced phase separation (TIPS) is a favorable method to fabricate polyolefin macroporous membranes [4–11]. PE, as a membrane material, possesses a wide range of desirable properties including excellent mechanical strength, thermal and physicochemical stability and low cost [4,12]. However, due to the hydrophobic nature and absence of polar functional groups in molecular

*Corresponding author.

chains of PE, the prepared membranes exhibit a low water flux and high fouling characteristic compared to other membranes made by hydrophilic polymers [12,13]. Actually, the hydrophobic membranes are susceptible to fouling while treating aqueous solutions containing natural organic matters (NOM), e.g. proteins and humic acids, which are prone to being easily absorbed onto the membrane surface or block the surface pores [14]. Therefore, the effective control of fouling is crucial for proper performance and long term effectiveness of any membrane system for water processing [16].

A great deal of efforts have been made to improve the hydrophilic characteristics of polymer membranes by applying different methods such as graft-polymerization with hydrophilic monomers, plasma technique for surface treatment, ozone treatment, blending and dip-coating [12,17,18]. Although the grafted surfaces are almost stable, chemicals used for grafting are sometimes environmentally unfriendly. Also, grafting by gamma ray and UV irradiation, or in the plasma chamber, is not easy to apply on a large industrial scale [15].

There are some inherently hydrophilic polymers like polyvinyl alcohol (PVA), polyacrylic acid (PAA), polyvinyl pyrrolidone (PVP), polyacrylonitrile (PAN) and PEG used to enhance the membranes hydrophilicity [14,19–22]. PEG, due to its hydrophilicity, good biocompatibility, low toxicity and cost has been widely investigated [21,23–25]. In this approach, the steric stabilization effect of PEG prevents proteins and other foulants from adhering to the surface [26,27]. However, most of the water soluble PEG may be washed out during membrane fabrication and also in filtration process. As reported in our previous work [28], grafting of PEG onto silica nanoparticles (NPs) is a promising approach to retain PEG in the membrane matrix and improve its hydrophilicity for a long time. However, it was not discussed in details in terms of dispersion and distribution of synthesized NPs in the membranes matrix.

Generally, the incorporation of nanomaterials into polymer matrices to form nanocomposite membranes has become an important area of research [29]. However, the ultimate properties of a polymer nanocomposite membranes are very much dependent on the dispersion of the NPs in the continuous phase, and the interfacial interaction between the surface of nano-scale filler and polymer matrix [30]. In our previous work [28], promising results were obtained in humic acid removal from water resources, however, the dispersibility as well as hydrophilic property of the prepared membranes were not much improved.

In general, the polar fillers have inherently low compatibility with non-polar polymers, especially hydrocarbons such as PP and PE [31–34]. The approach to improve the interaction between PE and silica NPs in the present work is through silane coupling agents that have the ability to form a durable bond between organic and inorganic materials.

Our previous findings [35] indicated that incorporation of PEG/vinyl grafted silica NPs (PEG/vinyl-g-silica) into PE matrix can be a promising strategy to improve both interfacial adhesion and hydrophilic characteristics of polymer composite. In continuation with our achieved protein repellent NPs, in this work PEG/vinyl-g-silica NPs embedded HDPE nanocomposite membranes were fabricated via combination of both melt blending and TIPS processes. The grafting reaction of vinyl functionalized NPs onto HDPE chains were carried out by using dicumyl peroxide (DCP) as a free radical initiator. Finally the fabricated membranes were evaluated in terms of structural and operating parameters and compared with the pure and PEG-g-silica NPs embedded HDPE membranes.

Although in-house fabricated pure and nanocomposite HDPE membrane may show lower water permeation compared to other commercial membranes, however, the main goal of this work is based on the introducing of our methodology in membrane modification, which is applicable to other available commercial membranes, too.

The structural characterization and performance of the fabricated membranes were investigated through using a set of analyses including FE-SEM, BSE, EDS, AFM, contact angle and pure water flux. Furthermore, the fouling characteristics of the membranes were examined during filtration of humic acid (HA) solution as one of the main constituents of normal foulants in water treatment process. Finally, the fouling mechanisms of the fabricated membranes were analyzed by using combined fouling models.

By the way, the existence of large pores in microfiltration (MF) membranes may result in a minimal retention of macromolecular HA; therefore, the impact of pre-coagulation with polyaluminium chloride (PAC) on the MF process performance, which is often called the coagulation-MF hybrid process,was also investigated.

2. Experimental

2.1. Materials

Ethanol (EtOH, 99.9%), ammonium hydroxide (NH_4OH, 25%) and tetraethylorthosilicate (TEOS, 98%) as cosolvent, catalyst and precursor, respectively, for synthesis of the silica NPs were purchased from Merck. PEG(MW: 200) as hydrophilic modifier and vinyltrimethoxysilane (VTMS) as a coupling agent were purchased from Sigma-Aldrich and Merck, respectively. The commercial grade of HDPE, (M_w ca. 119500 g/mol) was provided by Amirkabir Petrochemical Company of Iran and was used as received. Mineral oilas diluent and acetone as extractor were purchased from Acros Organics and Merck, respectively. HA as a common water contaminant was purchased from Sigma-Aldrichto study the fouling behavior of the membranes. PAC as the coagulant was purchased from Yixing Bluwat Chemicals Company. All the chemicals were used without further purification.

2.2. Synthesis of silica NPs

The bare, PEG and PEG/vinyl grafted silica NPs were synthesized by using one-pot one-step sol gel method as described in detail in our previous works [35, 36]. However, the fabrication method of PEG/vinyl grafted silica NPs, as a key material, was described concisely in this work, too. In this regard, VTMS was added dropwise to the reaction mixture containing certain amounts of EtOH, TEOS, ammonia and H_2O, after the primary solution became transparent. After 5 min, PEG was added to the prepared solution and mixing continued for 60 min. The obtained solution was

centrifuged at 12,000 rpm for 10 min and then rinsed by DI water and ethanol for several times to ensure the removal of unreacted materials. Finally, the particles were dried at 75°C for 24 h to obtain the final NPs.

According to the obtained results, in all experiments, the concentration of TEOS and ammonia were kept constant at 0.25 mol/L and 0.5 mol/L, respectively. Also, the molar ratios of H_2O/TEOS, PEG/TEOS and VTMS/TEOS, were kept constant at 38/1, 4/1 and 1/9, respectively.

2.3. Membrane fabrication

HDPE powder and the synthesized NPs were dried for at least 6 h at 75°C before being used in the membrane fabrication. The total fraction of solid matter in this study, containing HDPE with NPs loading of 0, 1 and 2 wt%, in the casting solution was held constant at 20 wt%.

Silica NPs/HDPE and PEG-g-silica NPs/HDPE nanocomposite membranes were fabricated by dispersing the NPs into mineral oil using sonication (Sonopuls HD 3200, Bandelin) for 1 h before the addition of polyethylene to the diluent-nanoparticle suspension and then melt-blended at 160°C for 90 min in a sealed glass vessel. The solution was then allowed to degas for 30 min and cast on a preheated glass sheet by using a doctor blade. The plate was immediately quenched in the water bath (30°C) to induce phase separation. In order to extract the mineral oil, the membrane was then immersed in acetone for 24 h. Finally it was dried at room temperature to remove acetone. A similar procedure was used to fabricate pure polyethylene membrane.

In order to fabricate PEG/vinyl-g-silica NPs/HDPE nanocomposite membranes, the melt compounding containing certain amounts of NPs and 0.06 wt.% DCP in HDPE were carried out in a laboratory batch internal mixer (Brabender W50 EHT) at 180 with a rotor speed of 60 rpm. The chamber volume was 55 cc and the filling factor was selected as 0.8. The prepared product were then cooled and used to fabricate nanocomposite membranes according to the previous described TIPS procedure.

2.4. FTIR analysis

The chemical structure of the samples was studied by Fourier transform infrared spectroscopy (FTIR) with a VERTEX 70 FTIR spectrometer (Bruker, Germany) in the range of 4000–400 cm^{-1}. The sample pellet of nanoparticles for FTIR test was prepared by mixing the particles with KBr.

2.5. FE-SEM micrographs and EDAX analysis

The morphology of the samples was investigated by using MIRA3 XM Field Emission Scanning Electron Microscopes (FE-SEM) from Tescan (USA). Nanoparticle samples for FE-SEM observation were prepared by dropping the particle suspension in water onto the SEM stub by using carbon adhesive. Also, the cross-section of the membrane samples was prepared by fracturing in liquid nitrogen. All samples were coated with gold by sputtering before observation to make them conductive.

Furthermore, FE-SEM device was equipped with dispersive X-ray analysis (EDAX) detector to identify the chemical composition as well as to inspect dispersion of NPs in the cross-section of the nanocomposite membranes.

2.6. Dispersibility of NPs

Generally, progress in fabrication of nanocomposite membranes has been limited by the types of nanomaterials that can be incorporated into polymer membranes for performance enhancement. This limitation is mainly due to difficulties in ensuring appropriate interactions between NPs and polymer to form nanocomposite membranes [29].

Since heavy elements (high atomic number) backscatter electrons stronger than light elements (low atomic number), and thus appear brighter in the image [37], in this work BSE images were used to detect contrast between areas with different chemical compositions to confirm the dispersibility of NPs in nanocomposite membranes.

2.7. Tensile strength measurement

Tensile strength, as a measure of mechanical properties, was determined at break point of membranes by using a tensile testing machine (STM-5, Santam). The samples were cut in 50 mm in length and 10 mm in width and stretched by the testing speed of 50 mm/min.

2.8. Contact angle measurement

The hydrophilicity of membranes was investigated by measuring the contact angle between membrane surface and water droplet by using a contact angle goniometer (PGX, Thwing-Albert Instrument Co.).

2.9. Pure water flux (PWF)

PWF tests were conducted at room temperature by using a dead-end filtration system with 5 cm^2 of membrane area. The feed was pressurized by a nitrogen cylinder attached to the feed reservoir. To minimize the compaction effect, the pre-wetted membranes were compacted for 30 min at 2 bar. Then the pressure was reduced to 1.5 bar and after reaching steady state, the permeate water was collected for a certain time and water flux was calculated through the following equation:

$$J_0 = \frac{V}{A \times \Delta t} \tag{1}$$

where J_0 is pure water flux ($L/m^2 \cdot h$), V is the permeate volume (L), A is the membrane area (m^2) and Δt is the permeate time (h).

2.10. Membrane fouling and rejection

The effects of synthesized NPs on the removal of HA and fouling behavior of the membranes were investigated. HA solution was prepared by dissolving 1 g of HA in 1 L of Milli-Q water. Solution pH was adjusted to 7.0 by addition of 0.1 M NaOH as needed. The solution was filtered through a 0.45 μm filter to remove particulates and stored in the refrigerator (4°C) before use. After measuring the

steady state pure water flux (recognized as J_0), the filtration continued with HA solution. The permeate readings were then periodically taken for every 10 min time interval throughout 280 min of filtration duration at the constant trans-membrane pressure of 1.5 bar. After 280 min of HA filtration, PWF of the membrane was measured and recorded as J_1. Then the membrane was rinsed with distilled water and the cake layer formed on the membrane was gently removed mechanically by a sponge. After rinsing, the PWF was measured again and labeled as J_2.

In the next series of experiments, in order to investigate the effect of pre-coagulation on humic acid removal, 0.34 g/L PAC (PAC/HA weight ratio = 1/3) was added to HA solution. The solution was rapidly mixed with coagulant and then the filtration was performed without being settled, simulating in-line coagulation. Hydraulic retention time in the rapid mixing tank was about 5 min. Then, the filtration procedure was carried out as described in the previous paragraph.

In order to evaluate the antifouling properties of the membranes in details, the reversible (RFR), irreversible (IFR) and total fouling (TFR) ratios of the membranes were calculated by using J_0, J_1 and J_2 through the following equations:

$$RFR = \left(\frac{J_2 - J_1}{J_0}\right) \times 100 \quad (2)$$

$$IFR = \left(\frac{J_0 - J_2}{J_0}\right) \times 100 \quad (3)$$

$$TFR = \left(\frac{J_0 - J_1}{J_0}\right) \times 100 \quad (4)$$

The fouling resistance ability of the fabricated membranes was investigated by measuring the flux recovery ratio (FRR) of each sample calculated as follows:

$$FRR = \left(\frac{J_2}{J_0}\right) \times 100 \quad (5)$$

In order to measure the membrane rejection, the HA concentrations of feed and permeate solutions were determined by using a UV spectrophotometer (Bio Quest CE2501) and the HA rejection of membrane was calculated by using Eq. (6):

$$R(\%) = \left(1 - \frac{C_p}{C_f}\right) \times 100 \quad (6)$$

where R (%) is the rejection percentage, C_p and C_f are permeate and feed concentrations.

Each experiment was repeated at least two times. In the experiments, all composite membrane samples were prepared from at least two replicate synthesis sets.

2.11. Fouling mechanisms analysis

In order to describe the mechanisms responsible for flux decline during the filtration of HA solution, the constant pressure combined fouling models were investigated. The combined models assume that the two individual fouling mechanisms are independent and will occur throughout the filtration [13]. A summary of constant pressure combined fouling models including the models, equations and fitted parameters generated by Bolton [38] is provided in Table 1.

To analyze the membranes fouling , the flux expressions were considered relative to the fouling mechanisms. For this purpose, the permeate volume per membrane area (m^3/m^2) versus time was plotted and the value of fitted parameters, listed in Table 1, was determined by using the least square method. Finally, the model that best described the experimental data suggests the most probable fouling mechanism responsible for the observed flux decline.

3. Results and discussion

3.1. Synthesis and characterization of NPs

In this work, FE-SEM images as well as FTIR analysis of synthesized NPs were shown and discussed; however, more detailed discussion and characterization including contact angle, XRD, protein adsorption, DLS, TGA and dispersibility of the bare and functionalized NPs are available in our previous works [35,36].

3.1.1. FE-SEM and FTIR analyses

Fig. 1 shows the FE-SEM images and FTIR analysis of synthesized NPs. It can be seen that the particles sizes decreased significantly in the presence of PEG (Fig. 1b) and VTMS (Fig. 1c).

Furthermore, in the presence of PEG and VTMS, the surface morphology changes from complete spherical of unmodified sample to sharp edge of grafted samples. According to Akbari et al. [35], it can be attributed to the impact of PEG and VTMS as stopping agents, which prevent complete formation of Si-O-Si at every place of silica NPs network, resulting in a significant decrease in the size of the particles.

As shown in the figure, FTIR analysis illustrated that in comparison with bare silica NPs, the PEG-g-silica NPs show new absorption peaks at 1460 and 2950–2800 cm^{-1}, corresponding to the stretching vibration of alkyl groups, in addition to the absorption peak of Si-O-Si at 1100–1000 cm^{-1}. Also, for PEG/vinyl-g-silica NPs, the extra peaks were observed at 1410 corresponding to Si–CH=CH_2 (vinyl group as reported by Yan et al. [39]), confirming simultaneous grafting of PEG and vinyl moieties on silica NPs.

3.2. Characterization of the fabricated membranes

3.2.1. Morphology of the membranes

Fig. 2 shows FE-SEM images of cross section of the fabricated membranes. It can be obviously seen that all membrane samples have a leafy structure characterized by randomly oriented connected polyethylene leaves similar to HDPE-mineral oil system as discussed by Lloyd et al. [40]. As shown in Fig. 2, membrane porosity increases by adding silica NPs. According to Jafarzadeh et al. [12], increasing the membrane porosity in the presence of NP scan be due to the heterogeneous nucleation effect of the particles. On the other hand, the

Table 1
Constant pressure combined models of membrane fouling

Model	Equation	Fitted parameters
Cake filtration[a] and complete blocking[b] mechanism (CFCBM)	$V = \frac{J_0}{K_b}\left(1-\exp\left(\frac{-K_b}{K_c J_0^2}\left(\sqrt{1+2K_c J_0^2 t}-1\right)\right)\right)$	K_c (s/m²), K_b (s⁻¹)
Cake filtration and intermediate blocking[c] mechanism (CFIBM)	$V = \frac{1}{K_i}\ln\left(1+\frac{K_i}{K_c J_0}\left(\left(1+2K_c J_0^2 t\right)^{\frac{1}{2}}-1\right)\right)$	K_c (s/m²), K_i (m⁻¹)
Complete blocking and standard blocking[d] mechanism (CBSBM)	$V = \frac{J_0}{K_b}\left(1-\exp\left(\frac{-2K_b t}{2+K_s J_0 t}\right)\right)$	K_b (s⁻¹), K_s (m⁻¹)
Intermediate blocking and standard blocking mechanism (IBSBM)	$V = \frac{1}{K_i}\ln\left(1+\frac{2K_i J_0 t}{2+K_s J_0 t}\right)$	K_i (m⁻¹), K_s (m⁻¹)
Cake filtration and standard blocking mechanism (CFSBM)	$V = \frac{2}{K_s}\left(\beta\cos\left(\frac{2\pi}{3}-\frac{1}{3}\arccos(\alpha)\right)+\frac{1}{3}\right)$, $\alpha = \frac{8}{27\beta^3}+\frac{4K_s}{3\beta^3 K_c J_0}-\frac{4K_s^2 t}{3\beta^3 K_c}$, $\beta = \sqrt{\frac{4}{9}+\frac{4K_s}{3K_c J_0}+\frac{2K_s^2 t}{3K_c}}$	K_c (s/m²), K_s (m⁻¹)

[a]Cake filtration: Particles diameter is larger than membrane pores diameter, so fouling occurs due to cake formation on the membrane surface.
[b]Complete blocking: Each particle arriving at the membrane surface will block some pores.
[c]Intermediate blocking: Particles are accumulated on each other and sealed membrane pores.
[d]Standard blocking: Particles diameter is much less than membrane pore diameter, hence they can enter the pores and are adsorbed on the pore walls.

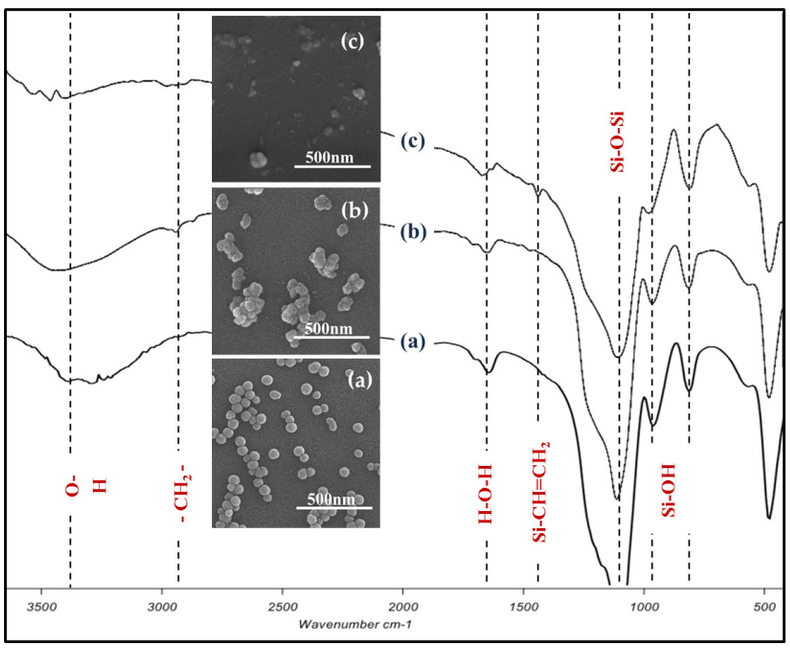

Fig. 1. FE-SEM and FTIR analyses of synthesized NPs; [NH_4OH] = 0.5 mol/L; PEG/TEOS and VTMS/TEOS molar ratio, respectively = (a) 0 and 0, (b) 1/4 and 0, (c) 1/4 and 1/9.

presence of silica NPs during phase separation gives rise to a greater nucleation rate and subsequently a shorter growth period of polyethylene leaves. Therefore, as shown in FE-SEM images (Fig. 2), smaller leaves are developed in the polymer matrix that causes the membrane to be more porous.

However, in the presence of vinyl grafted NPs (Fig. 2h and 2j) a different structure was obtained. The structure obtained for these samples in addition to the leafy structure similar to others,is an interconnected structure with interwoven polyethylene fibers. The presence of these

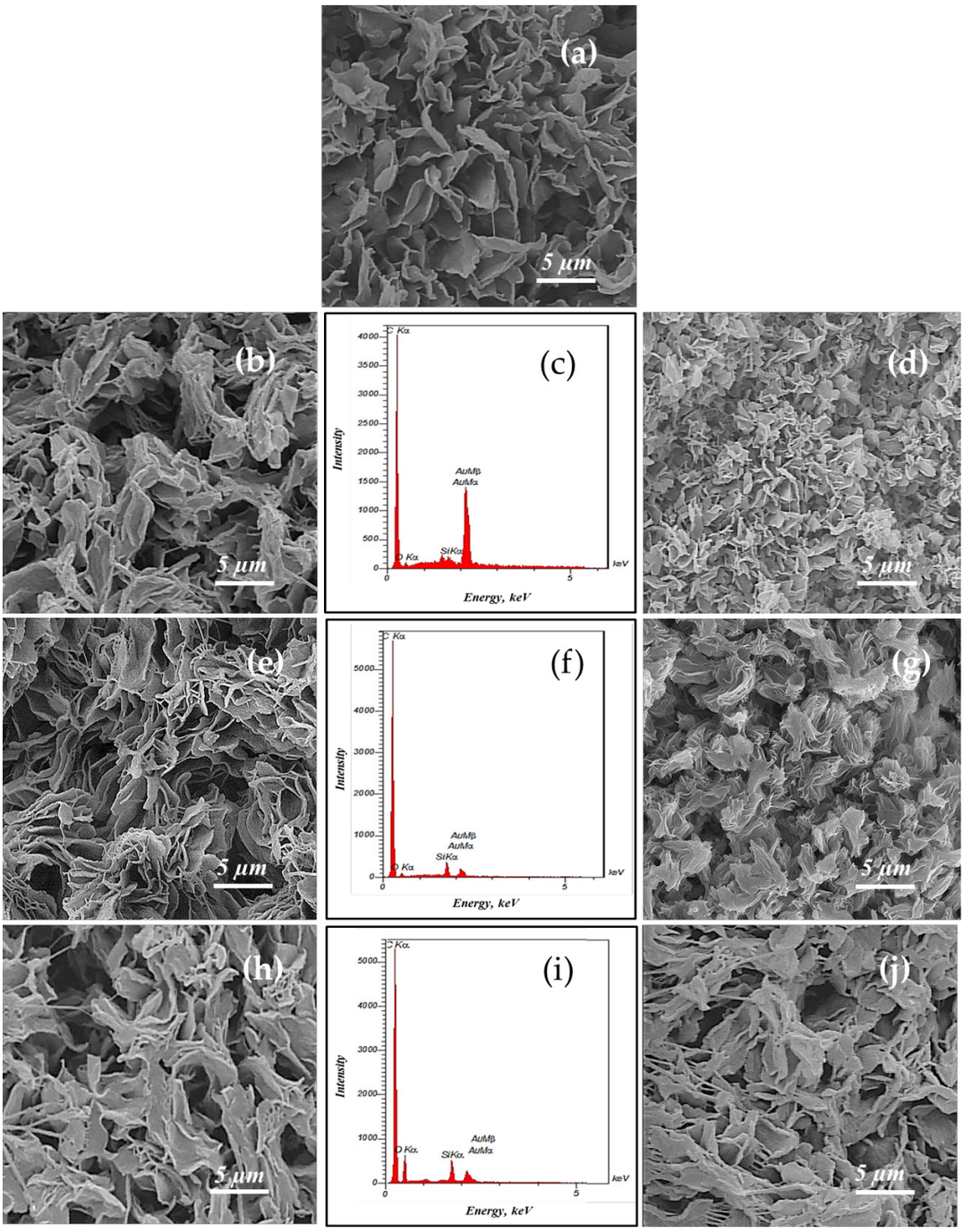

Fig. 2. FE-SEM images and EDS analysis of neat and nanocomposite HDPE membranes cross section; (a) Pure HDPE membrane, (b) and (c) 1 wt.% bare silica NPs/HDPE membrane, (d) 2 wt.% bare silica NPs/HDPE membrane, (e) and (f) 1 wt.% PEG-g-silica NPs/HDPE membrane, (g) 2 wt.% PEG-g-silica NPs membrane, (h) and (i) 1 wt.% PEG/vinyl-g-silica NPs/HDPE membrane, (j) 2 wt.% PEG/vinyl-g-silica NPs/HDPE membrane.

interwoven fibers at 2 wt.% loading of vinyl grafted NPs (Fig. 2j) is quite evident and could affect the membrane porosity and change the final structure. The appearance of this structure can be due to the desirable interaction between HDPE chains and vinyl moieties of particles in the presence of initiator.

EDS analysis of the samples containing 1 wt.% NPs, as case study examples, gave the composition of the nanocomposite membranes as shown in Fig. 2c, 2f and 2i. The elemental analysis reveals the presence of Si and O in the membranes. The Au peak in the spectrum comes from treating the samples with Au sputtering.

In order to study the dispersibility of NPs throughout the membranes, EDAX analysis was carried out. The FE-SEM images and EDAX analysis of membranes cross-section for samples with 2 wt.% loading of NPs are shown in Fig. 3. As shown in the figure, all membranes have symmetric structure with homogeneous morphology. Based on EDAX analysis, agglomeration of the bare and PEG grafted silica NPs into membranes matrix, due to

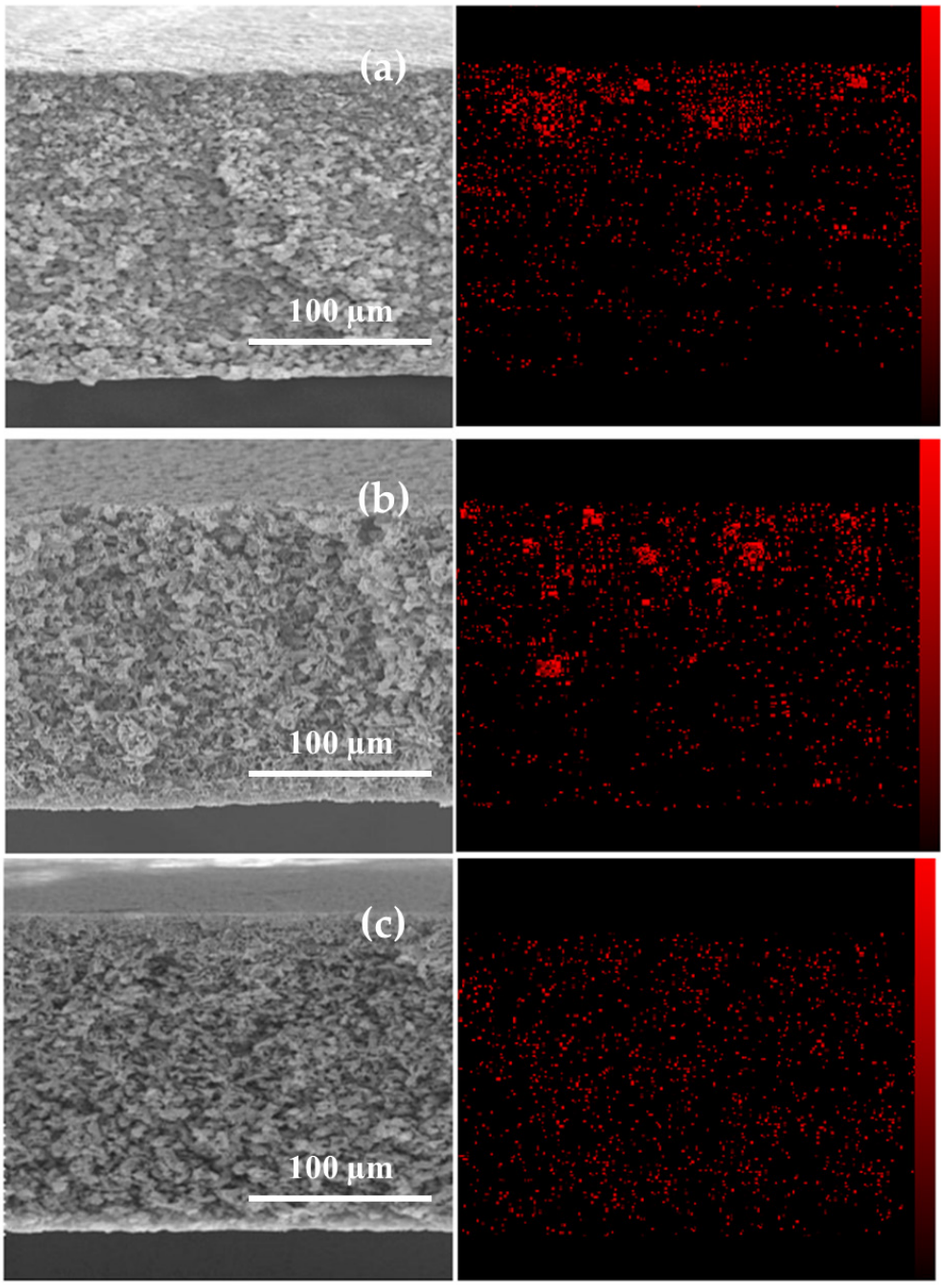

Fig. 3. FE-SEM images and EDAX analysis of cross-section; (a) 2 wt.% bare silica NPs/HDPE membrane, (b) 2 wt.% PEG-g-silica NPs membrane, (c) 2 wt.% PEG/vinyl-g-silica NPs/HDPE membrane.

poor interaction between NPs and polymer chains, is quite visible. However, a good dispersion can be seen in the case of vinyl grafted particles. Indeed, as discussed by Akbari et al. [35], the bifunctional structures of VTMS (used in this work as a coupling agent) containing vinyl (R-CH=CH_2) and alkoxy (R-O (R: CH_3 or CH_2CH_3)) functional groups, make it possible for them to be grafted onto polyethylene backbones and be coupled with hydrolysable groups of silica NPs via condensation, respectively. Therefore, a high dispersibility could be achieved in the presence of vinyl moieties due to significant improvement in interaction between synthesized NPs and HDPE chains.

3.2.2. BSE analysis

Fig. 4 shows BSE images of HDPE nanocomposite membranes that were acquired from acceleration voltage of 15 kV. As shown in the images, the dense bright spots represented the response from NPs on and just underneath the surface of membranes.

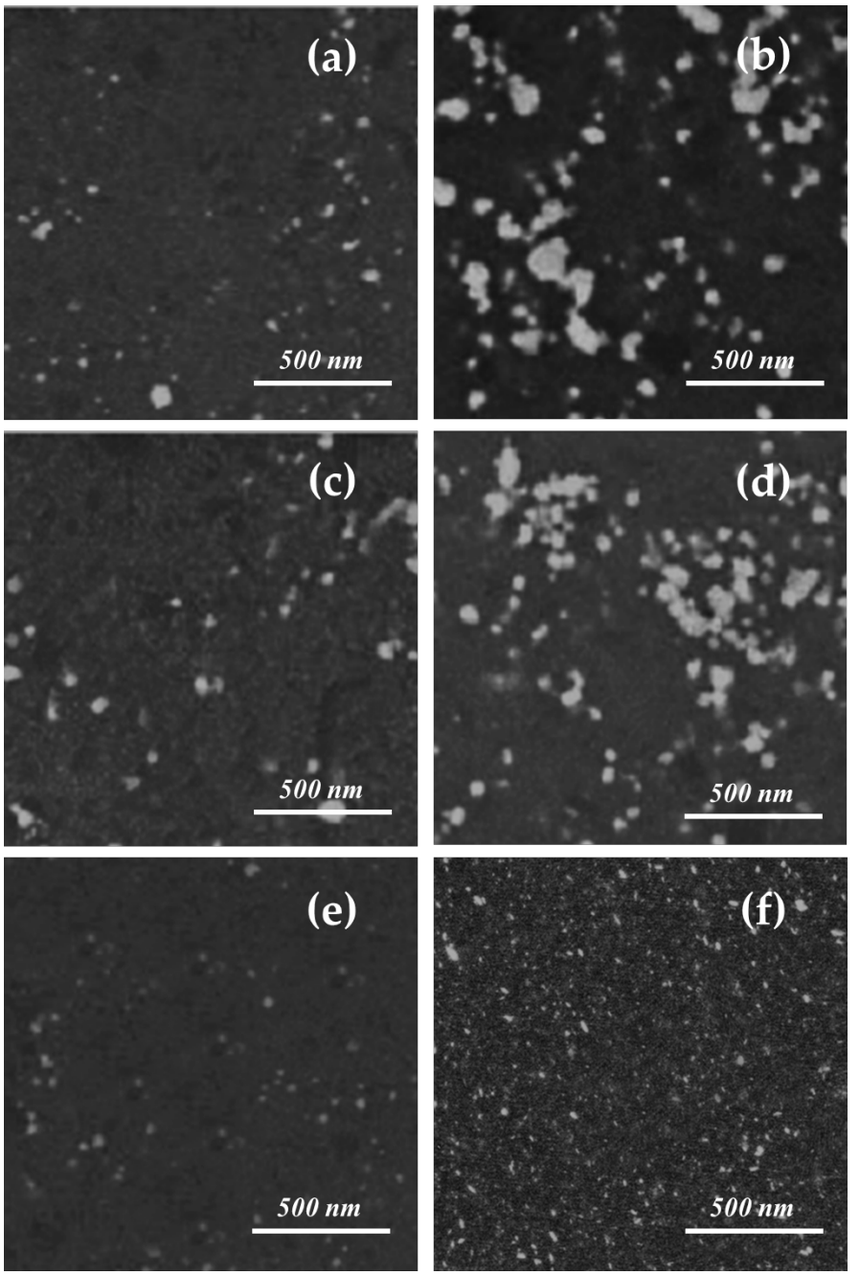

Fig. 4. BSE images of HDPE nanocomposite membranes: (a) 1 wt.% bare silica NPs/HDPE membrane, (b) 2 wt.% bare silica NPs/HDPE membrane, (c) 1 wt.% PEG-g-silica NPs/HDPE membrane, (d) 2 wt.% PEG-g-silica NPs membrane, (e) 1 wt.% PEG/vinyl-g-silica NPs/HDPE membrane, (f) 2 wt.% PEG/vinyl-g-silica NPs/HDPE membrane.

The results obtained from BSE images (similar to EDAX analysis, Fig. 3) show that the bare and PEG grafted silica NPs agglomerated within HDPE membranes matrix due to the lack of interaction between NPs and polymer matrix (Fig. 4a, 4c and 4e). It should be mentioned that the agglomeration of NPs become more clear at higher loading of NPs (2 wt.%). However, dispersibility was improved by grafting vinyl moieties onto silica NPs leading to an effective dispersion in the polymer matrix (Fig. 4e and 4f).

3.2.3. PWF measurement

The obtained results from PWF measurement are shown in Fig. 5. Pure HDPE membrane had the lowest flux, about 11 $L \cdot m^{-2} h^{-1}$, among the fabricated membranes. However, water flux increased in the presence of synthesized NPs. Grafting of PEG as a hydrophilic agent onto the silica particles was significantly effective in increasing the membrane flux at 1 wt.% loading of NPs (82 $L \cdot m^{-2} h^{-1}$), as discussed in our previous work [28]. Nevertheless, by increasing the concentration of NPs to 2 wt.%, a significant reduction in PWF can be seen for membranes containing bare and PEG grafted silica NPs. Generally, at higher loading of NPs the possibility of particles agglomeration within membrane matrix will increase if there is no sufficient interaction between particles and polymer chains. Therefore, the presence of agglomerated bare and PEG grafted silica NPs within the polymer matrix, caused to block of some membrane pores.

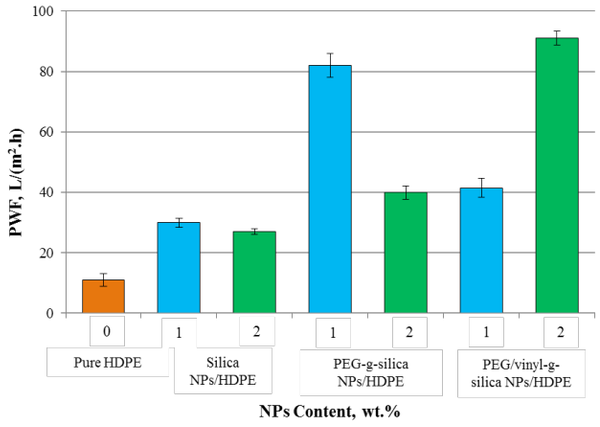

Fig. 5. PWF of fabricated membranes including; Pure HDPE membrane, Silica NPs/HDPE membrane, PEG-g-silica NPs/HDPE membrane and PEG/vinyl-g-silica NPs/HDPE membrane.

However, desirable dispersion of NPs in the presence of vinyl silane functional group caused an increase in the PWF to more than 90 $L \cdot m^{-2} h^{-1}$. In fact, in addition to hydrophilicity, improving the dispersibility of NPs within membrane matrix has a significant impact on increasing the membrane flux.

It is worth to note that despite of lower water permeation of in-house fabricated HDPE membrane compared to other commercial available one, the main goal in this work is to present our approach in modification of membranes performance.

Since the surface structure plays an important role in the membrane flux, the surfaces of nanocomposite membranes containing 2 wt.% NPs were investigated by using FE-SEM analysis (Fig. 6). As shown in Fig. 6, no significant difference is observed in the membrane surface structure for silica NPs/HDPE and PEG-g-silica NPs/HDPE membranes. However, in the presence of vinyl functionalized particles, the interconnected structure with interwoven polyethylene fibers can be seen. It should be mentioned that this structure is similar to the structure observed for the cross section of this sample (Fig. 2j).

3.2.4. Tensile strength of membranes

Fig. 7. shows the normalized tensile strengths of fabricated membranes on the basis of pure HDPE strength. It can be seen that the tensile strength in nanocomposite membranes is higher than in pure HDPE membrane, mainly due to the reinforcement effect of inorganic particles. In fact, the dispersion of NPs in the membranes matrix acts as physical cross-links to bear the stress of the load and therefore improve the membrane tensile strength [41]. However, there is a considerable difference in tensile strength between the membranes in the presence and absence of vinyl moieties, and as can be

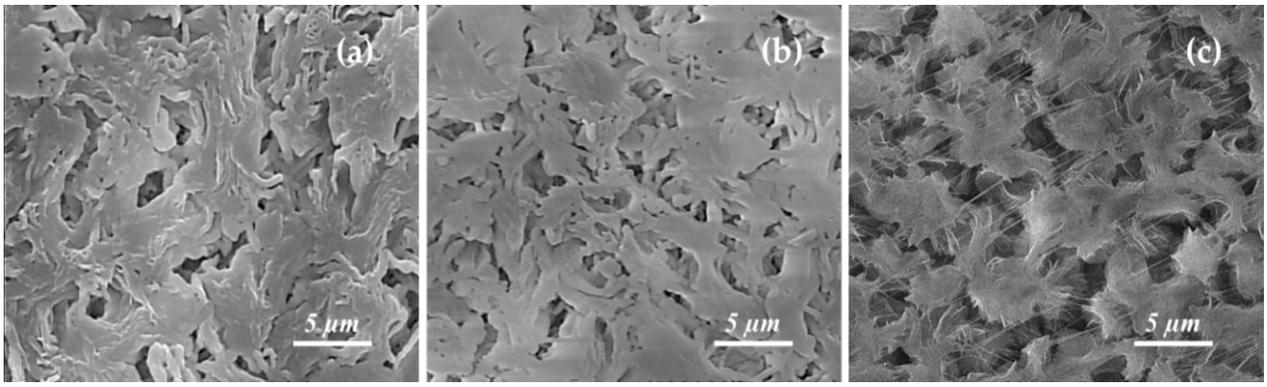

Fig. 6. FE-SEM images of membranes surface; (a) 2 wt.% bare silica NPs/HDPE membrane, (b) 2 wt.% PEG-g-silica NPs membrane, (c) 2 wt.% PEG/vinyl-g-silica NPs/HDPE membrane.

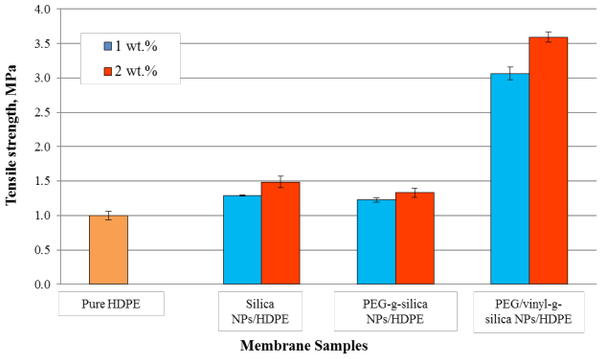

Fig. 7. Tensile strength of fabricated membranes including Pure HDPE membrane, Silica NPs/HDPE membrane and PEG-g-silica NPs/HDPE membrane and PEG/vinyl-g-silica NPs/HDPE membrane.

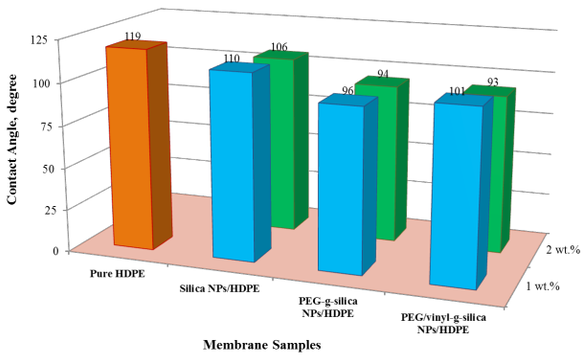

Fig. 8. Contact angles of fabricated membranes including Pure HDPE membrane, Silica NPs/HDPE membrane and PEG-g-silica NPs/HDPE membrane and PEG/vinyl-g-silica NPs/HDPE membrane.

seen, the nanocomposite membrane containing 2 wt.% PEG/vinyl-g-silica NPs exhibits the highest tensile strength (about 3.6 times higher than that of pure HDPE membrane). According to FE-SEM images (Figs. 2 and 6), existence of the interconnected structure with interwoven polyethylene fibers in the presence of vinyl functionalized NPs may significantly increase the tensile strength of this sample.

3.2.5. Contact angle measurement

Fig. 8 shows the contact angle measurements for the outer surfaces of the fabricated membranes. As expected, there is a significant reduction in the contact angle of HDPE membrane in the presence of synthesized NPs. For silica NPs/HDPE membrane, a certain amounts of hydroxyl groups on the SiO_2 particles made membrane more hydrophilic than pure HDPE. Furthermore, comparing the contact angle of nanocomposite membranes containing 1 wt.% NPs confirms that the PEG-g-silica NPs/HDPE membrane is more hydrophilic than other samples due to the inherent hydrophilic characteristic of PEG.

As discussed by Akbari et al. [35], the main problem with PEG-g-silica NPs/HDPE nanocomposite is the agglomeration of particles during compounding processing. It is practically difficult to produce a monodispersed HDPE nanocomposite matrix because of NPs agglomeration due to the lack of sufficient interaction between NPs and HDPE matrix. This problem could be easily overcome by modifying PEG-g-silica NPs in the presence of vinyl moieties as a coupling agent. As shown in Fig. 8, the hydrophilicity of the membranes was improved in the presence of 2 wt.% PEG/vinyl-g-silica NPs (93 degree). Comparing the samples with and without vinyl moieties confirms the impact of effective dispersion of NPs within polymer matrix on the improvement of membranes' hydrophilicity in the presence of vinyl functionalized NPs.

3.2.6. Flux decline during HA filtration

Fig. 9 shows the membranes flux decline during HA filtration. The flux of pure HDPE membrane after about 120 min was almost zero. It can be seen that the flux increases significantly in the presence of synthesized NPs, compared

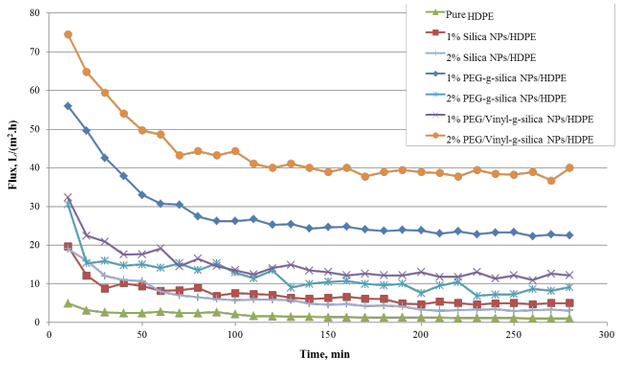

Fig. 9. Flux-time behavior of pure and nanocomposite HDPE membranes during filtration of 1 g/L HA solution.

with pure HDPE. At constant weight fraction of 1 wt.% NPs, PEG-g-silica NPs/HDPE membrane shows a higher flux during filtration process than others. It may be due to the inherent hydrophilicity of PEG that makes the HDPE membrane more permeable as discussed in details in our previous work [28]. However, it should be mentioned that in addition to the presence of NPs, changing of the membrane structure (shown in Fig. 6) could effective in trend of flux decline during filtration. Similar to PWF analysis, the performance of vinyl grafted NPs/HDPE membrane has become much better than other samples at a higher dosage of particles (2 wt.%). According to BSE images, as discussed earlier, by increasing the concentration of NPs in casting solution, particles tend to agglomerate/aggregate. Indeed, at higher loading of NPs, dispersibility plays a crucial role in the final performance of the membrane. Therefore, simultaneously improving both hydrophilicity and dispersibility of NPs (for PEG/vinyl-g-silica NPs sample) could in turn improve membrane PWF even at higher dosages of NPs.

3.2.7. Fouling analysis and membranes performance

According to the experimental fouling data substituted in the linearized equations of combined fouling models, the

obtained values of fitted parameters and correlation coefficient (R^2) for pure and nanocomposite membranes are listed in Table 2.

Figs. 10–12 illustrate the graphs obtained from experimental data and predicted mechanisms for flux decline during filtration process. As shown in Fig. 10, it can be concluded that for pure HDPE membrane, the best fit of data occurred with both of CFCBM and CFSBM models.

The results obtained from combined fouling models for nanocomposite membranes containing 1 wt.% NPs is shown in Fig. 11. Compared to pure HDPE membrane, the best fit of data for silica and PEG-g-silica NPs/HDPE membranes was observed only in CFCBM model.

However, for 1 wt.% vinyl grafted NPs/HDPE nanocomposite membrane in addition to CFCBM, CFSBM occurred as well. It is interesting to mention that complete blocking and cake filtration, which occurred on the membrane surface, are types of reversible fouling that could be removed by physical cleaning methods. However, standard blocking is a kind of irreversible fouling due to accumulation of particles on the walls of pores, inside of the membranes [28].

Fig. 12 shows the results obtained from the combined fouling models for nanocomposite membranes containing 2 wt.% NPs.

Contrary to previous results (Fig. 11), by increasing the concentration of NPs dispersed in membrane matrix,vinyl

Table 2
Model parameters, regression coefficient and error of fit for constant pressure combined models of membrane fouling

Membrane samples		Models	Fitted parameters				R^2
			k_s (m^{-1})	k_i (m^{-1})	k_c (min/m^2)	k_b (min^{-1})	
Pure HDPE membrane		CFCBM			6.42E + 06	4.91E-04	0.9899
		CFIBM		19.71	5.59E + 06		0.9855
		CFSBM	77.03		6.09E + 06		0.9898
		CBSBM	132.8			0.01686	0.8159
		IBSBM	3.479	375.4			0.9161
Silica NPs/HDPE nanocomposite membrane	1 wt.%	CFCBM			4.04E + 05	3.07E-08	0.9912
		CFIBM		84.42	4.09E + 01		0.9428
		CFSBM	55.77		5.88E + 01		0.8824
		CBSBM	53.03			1.43E-03	0.8823
		IBSBM	1.167	81.68			0.9381
	2 wt.%	CFCBM			3.07E + 05	5.34E-03	0.9997
		CFIBM		88.43	0.01558		0.9911
		CFSBM	40.94		2.77E + 05		0.9998
		CBSBM	57.98			4.05E-04	0.9583
		IBSBM	6.08E-01	86.07			0.9902
PEG-g-silica NPs/HDPE nanocomposite membrane	1 wt.%	CFCBM			1.36E + 04	4.95E-03	0.9670
		CFIBM		17.55	1.034		0.9543
		CFSBM	12.55		1.13E + 02		0.9193
		CBSBM	12.44			1.93E-04	0.9186
		IBSBM	2.66E-07	17.56			0.9543
	2 wt.%	CFCBM			1.39E + 05	3.82E-05	0.9910
		CFIBM		43.93	1.008		0.9567
		CFSBM	0.008946		1.40E + 05		0.991
		CBSBM	30.61			2.66E-05	0.9169
		IBSBM	3.06E-02	43.87			0.9566
PEG/vinyl-g-silica NPs/HDPE nanocomposite membrane	1 wt.%	CFCBM			8.69E + 04	5.74E-07	0.9891
		CFIBM		31.45	29.83		0.9602
		CFSBM	0.339		8.64E + 04		0.9891
		CBSBM	22.96			6.42E-06	0.9300
		IBSBM	1.16E-03	31.49			0.9603
	2 wt.%	CFCBM			8.02E + 03	1.34E-07	0.9894
		CFIBM		7.708	35.26		0.9743
		CFSBM	6.4		3.47E + 02		0.9604
		CBSBM	6.15			4.67E-05	0.9611
		IBSBM	1.00E-05	7.796			0.9745

grafted particles shows better performance due to good dispersibility. As shown in Fig. 12, for PEG/vinyl-g-silica NPs/HDPE membrane containing 2 wt.% NPs, the best fit of data was observed only in CFCBM model. However,

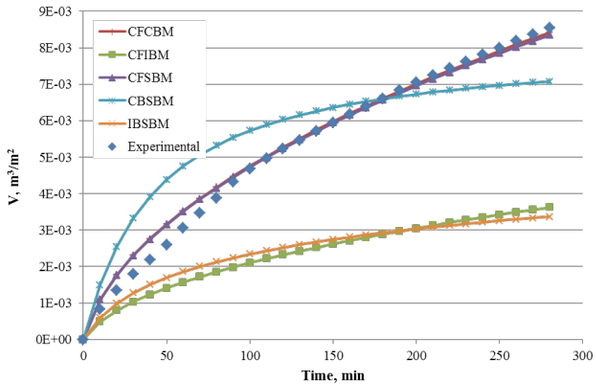

Fig. 10. Experimental filtrated volume data compared to the combined fouling models for pure HDPE membrane during filtration of HA solution.

for silica and PEG-g-silica NPs/HDPE membranes both of CFCBM and CFSBM occurred.

It means that, for membranes at a lower loading of NPs in which the dispersibility may not be a critical problem, grafting of vinyl moieties on NPs could not significantly help to improve the membrane performance. However, at a higher loading of NPs, dispersibility should be considered as a crucial parameter in the final performance of membranes.

In order to analyze the fouling behavior of the fabricated membranes in further details,the reversible, irreversible and total fouling ratios of pure and nanocomposite HDPE membranes were investigated and the obtained results are summarized in Table 3.

The pure HDPE membrane exhibited the highest TFR (88.18%) and IFR (52.64%) values. However, NPs loading improved the antifouling behavior of the membranes, in which a decrease in TFR and IFR and an increase in RFR values were observed.

The RFR of PEG/vinyl-g-silica NPs/HDPE membrane increased significantly by increasing the amount of particles to 2 wt.%, which led to a reduction in the IFR. This is probably due to enhanced hydrophilicity and good dispersion of the NPs through simultaneous presence of PEG as well as vinyl moieties which prevented the direct contact between

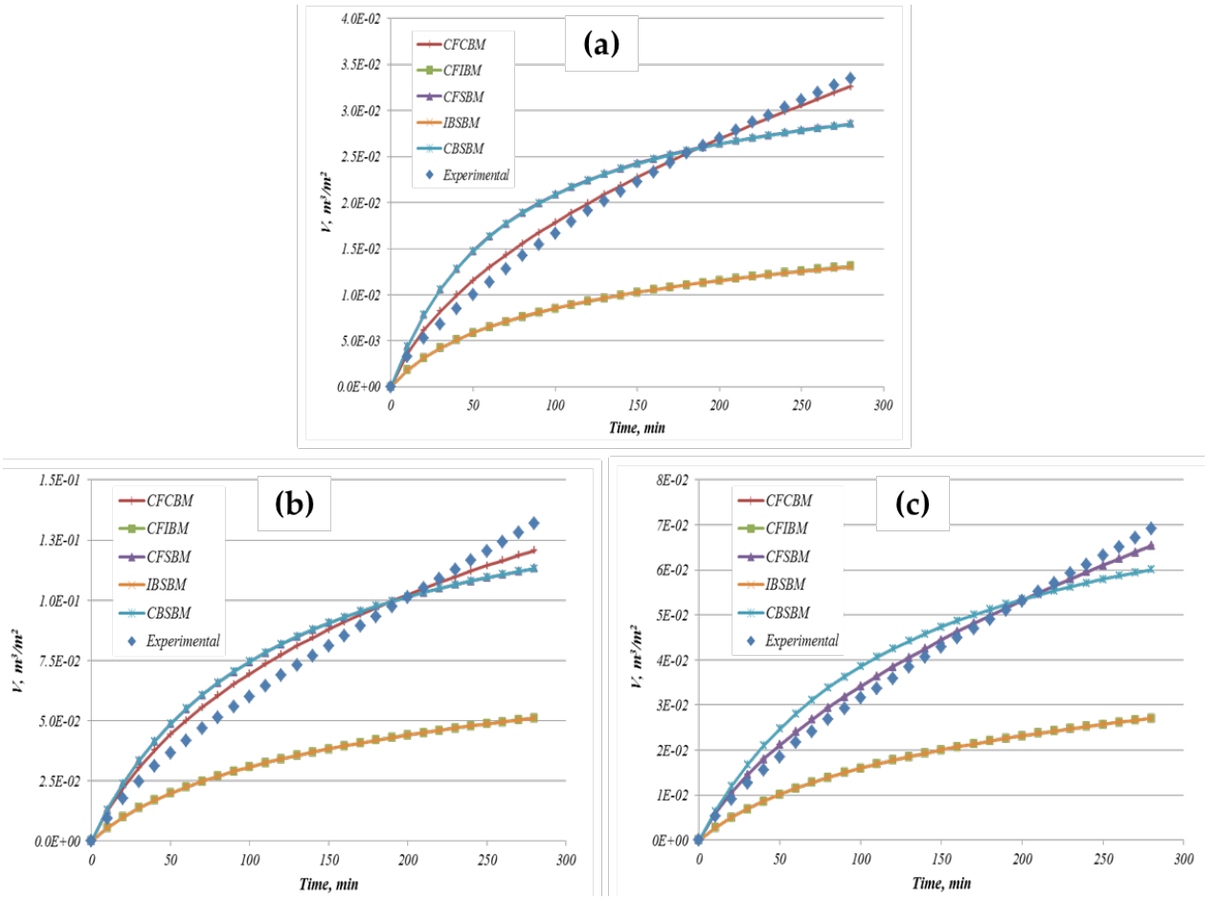

Fig. 11. Experimental filtrated volume data compared to the combined fouling models for 1 wt.% NPs embedded membranes during filtration of HA solution. (a) bare silica NPs/HDPE membrane, (b) PEG-g-silica NPs membrane, (c) PEG/vinyl-g-silica NPs/HDPE membrane.

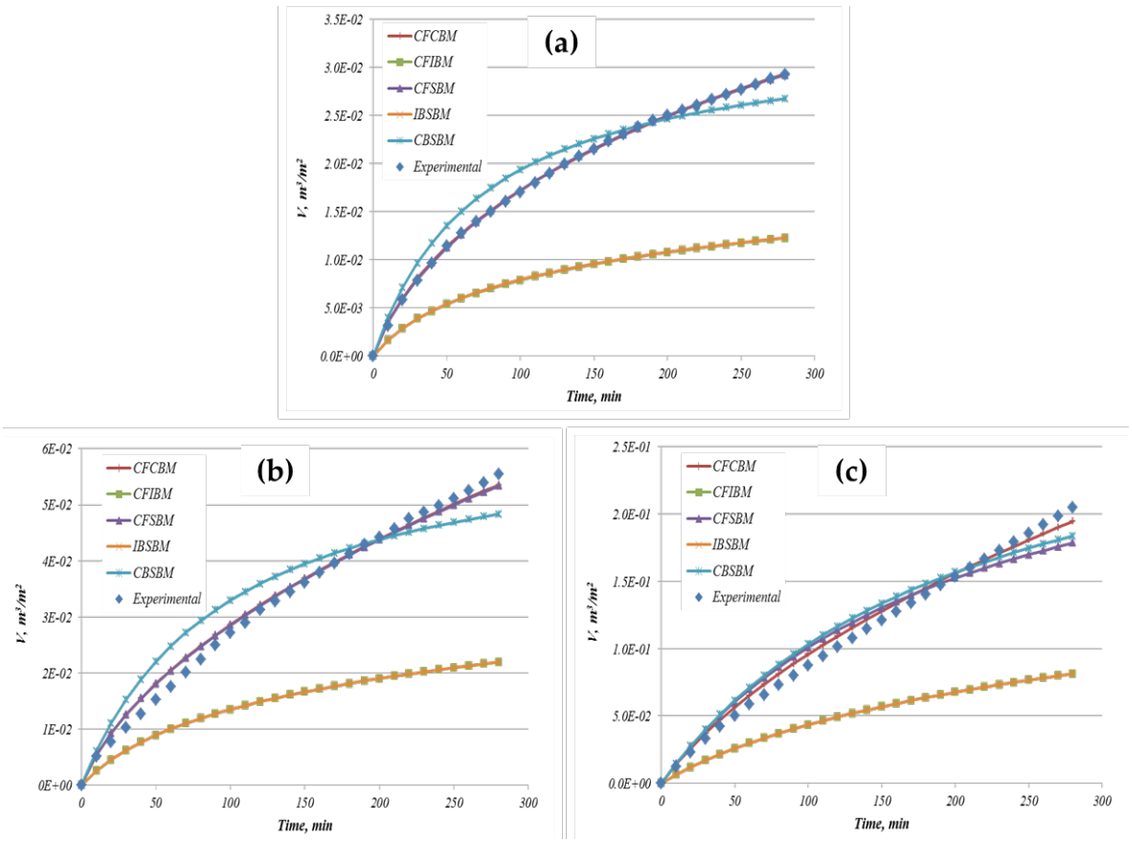

Fig. 12. Experimental filtrated volume data compared to the combined fouling models for 2 wt.% NPs embedded membranes during filtration of HA solution. (a) bare silica NPs/HDPE membrane, (b) PEG-g-silica NPs membrane, (c) PEG/vinyl-g-silica NPs/HDPE membrane.

Table 3
Fouling parameters of prepared membranes during HA filtration; TFR: total fouling ratio; RFR: reversible fouling ratio and IFR: irreversible fouling ratio

Membrane Samples		RFR (%)	IFR (%)	TFR (%)
Pure HDPE membrane	–	35.55	52.64	88.18
Silica NPs/HDPE membrane	1 wt.%	43.53	39.93	83.47
	2 wt.%	33.33	51.85	85.19
PEG-g-silica NPs/HDPE membrane	1 wt.%	51.59	18.98	70.57
	2 wt.%	35.09	37.34	72.43
PEG/vinyl-g-silica NPs/HDPE membrane	1 wt.%	38.58	30.07	68.65
	2 wt.%	43.83	15.46	59.29

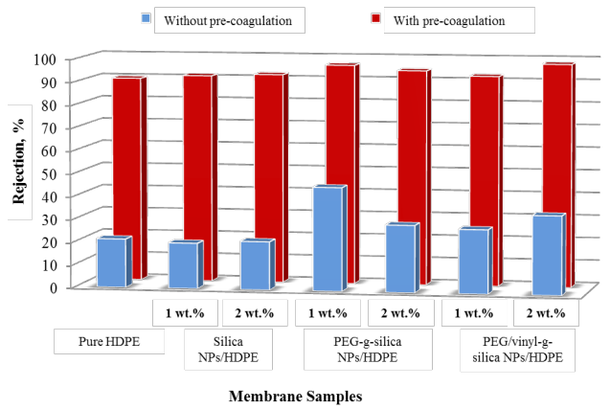

Fig. 13. Rejection performance of fabricated membranes with and without pre-coagulation process.

the foulants and the membrane. However, the inverse trend can be observed for membranes containing silica and PEG-g-silica NPs.

Fig. 13 shows the results of rejection test that were calculated by using Eq. (6) for membrane samples with and without coagulation pre-treatment during filtration of HA. In addition, the values of flux recovery ratio measured with and without pre-coagulation are shown in Fig. 14. There are large discrepancies in the trend of membranes rejections between the cases with and without coagulation pre-treatment. According to Figs. 13 and 14, pre-coagulation of feed water with PAC improves the HA removal as well as mem-

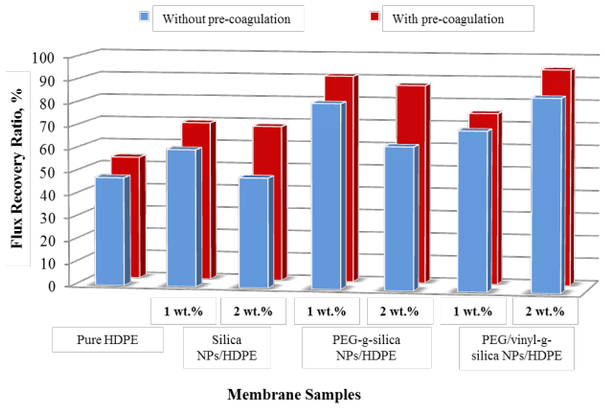

Fig. 14. Flux recovery ratios of fabricated membranes with and without pre-coagulation process.

brane flux recovery for all samples. In other words, combination of the MF HDPE membranes with physicochemical coagulation process not only could reduce membrane fouling but also improves the quality of the produced water.

Particle destabilization by charge neutralization and sweep coagulation has been considered as two main mechanisms, explaining the flocculation of HA by metal coagulants [42,43]. Both mechanisms increase the HA particle size and accordingly result in a better removal of HA and a decrease in the membranes fouling. However, as discussed by Akbari et al. [28], according to the pH value adjusted in this study (pH = 7), sweep-floc condition is the dominant mechanism for improving the membrane performance after pre-coagulation.

As shown in Fig. 14, the flux recovery of all samples shows similar trends in terms of PWF and flux recovery. The best flux recovery was observed for 2 wt.% vinyl grafted NPs embedded membrane (95%) after pre-coagulation. However, flux recovery values for silica as well as PEG-g-silica NPs embedded membranes decreased by increasing the NPs loading from 1 wt.% to 2 wt.%, that might be due to particles agglomeration within membrane matrix as discussed earlier.

4. Conclusions

Developing the antifouling membranes is still highly demanded for widespread application of membranes. Accordingly, the synthesis of hydrophilic as well as highly dispersible nanofillers by grafting particular functional groups can be a helpful strategy to efficiently tailor the hydrophilic property, desired morphology, good permeability, high rejection and less fouling characteristics to polymer membranes. One might quibble that in-house prepared HDPE membranes exhibit lower PWF compared to commercial membranes, however, the main goal was based on the introducing of our novel and unique approach in membrane modification, which is applicable to other available commercial membranes.

In this work, we focused on improving the permeability, mechanical strength and antifouling properties of HDPE membranes by embedding PEG/vinyl grafted NPs into polymer matrix. By improving the interaction between NPs and HDPE, efficient foulant repellent characteristics as well as high interfacial adhesion between NPs and HDPE polymer were achieved. The obtained results were evaluated by using several structural and operational analyses including FE-SEM, EDAX, BSE, contact angle, tensile strength and PWF. Furthermore, the fouling mechanisms were investigated to confirm the significant impacts of functionalized NPs on the efficient performance of nanocomposite HDPE membranes.

References

[1] J.H. Jhaveri, Z.V.P. Murthy, A comprehensive review on anti-fouling nanocomposite membranes for pressure driven membrane separation processes, Desalination, 379 (2016) 137–154.
[2] A. Akbari, R. Yegani, Study on the impact of polymer concentration and coagulation bath temperature on the porosity of polyethylene membranes fabricated via TIPS method, J. Membr. Sep. Technol., 1 (2012) 100–107.
[3] M. Ahsani, R. Yegani, Study on the fouling behavior of silica nanocomposite modified polypropylene membrane in purification of collagen protein, Chem. Eng. Res. Des., 102 (2015) 261–273.
[4] C. Zhang, Y. Bai, Y. Sun, J. Gu, Y. Xu, Preparation of hydrophilic HDPE porous membranes via thermally induced phase separation by blending of amphiphilic PE-b-PEG copolymer, J. Membr. Sci., 365 (2011) 216–224.
[5] H. Matsuyama, H. Okafuji, T. Maki, M. Teramoto, N. Kubota, Preparation of polyethylene hollow fiber membrane via thermally induced phase separation, J. Membr. Sci., 223 (2003) 119–126.
[6] M. Shang, H. Matsuyama, M. Teramoto, D.R. Lloyd, N. Kubota, Preparation and membrane performance of poly(ethylene-co-vinyl alcohol) hollow fiber membrane via thermally induced phase separation, Polymer, 44 (2003) 7441–7447.
[7] H. Matsuyama, S. Berghmans, D.R. Lloyd, Formation of hydrophilic microporous membranes via thermally induced phase separation, J. Membr. Sci., 142 (1998) 213–224.
[8] J.A.i. de Lima, M.I. Felisberti, Porous polymer structures obtained via the TIPS process from EVOH/PMMA/DMF solutions, J. Membr. Sci., 344 (2009) 237–243.
[9] A. Akbari, R. Yegani, Y. Jafarzadeh, A. Dadgostar, Application of full factorial experimental design to investigate the impact of polymer concentration and coagulation bath temperature in fabrication of microporous PE membranes via TIPS method, in: The 7th Conference of Aseanian Membrane Society, Busan, Korea, 2012.
[10] Z. Wang, W. Yu, C. Zhou, Preparation of polyethylene microporous membranes with high water permeability from thermally induced multiple phase transitions, Polymer, 56 (2015) 535–544.
[11] A. Akbari, R. Yegani, A. Behboudi, Study on the impact of coagulation bath temperature on the surface morphology and performance of polyethylene membrane prepared by TIPS method in purification of collagen protein, Iran. J. Polym. Sci. Technol, 28 (2015) 395–407.
[12] Y. Jafarzadeh, R. Yegani, M. Sedaghat, Preparation, characterization and fouling analysis of ZnO/polyethylene hybrid membranes for collagen separation, Chem. Eng. Res. Des., 94 (2015) 417–427.
[13] Y. Jafarzadeh, R. Yegani, Analysis of fouling mechanisms in TiO2 embedded high density polyethylene membranes for collagen separation, Chem. Eng. Res. Des., 93 (2015) 684–695.
[14] G.-d. Kang, Y.-m. Cao, Application and modification of poly(vinylidene fluoride) (PVDF) membranes – A review, J. Membr. Sci., 463 (2014) 145–165.
[15] D. Rana, T. Matsuura, Surface modifications for antifouling membranes, Chem. Rev. (Washington, DC, U. S.), 110 (2010) 2448–2471.

[16] G.-d. Kang, Y.-m. Cao, Development of antifouling reverse osmosis membranes for water treatment: A review, Water Res., 46 (2012) 584–600.
[17] Y.-R. Qiu, H. Matsuyama, G.-Y. Gao, Y.-W. Ou, C. Miao, Effects of diluent molecular weight on the performance of hydrophilic poly(vinyl butyral)/Pluronic F127 blend hollow fiber membrane via thermally induced phase separation, J. Membr. Sci., 338 (2009) 128–134.
[18] Z. Shoeyb, R. Yegani, E. Shokri, Preparation and characterization of HDPE/EVA flat sheet membranes by thermally induced phase separation method, Iran. J. Polym. Sci. Technol., 28 (2015) 149–159.
[19] B. Chakrabarty, A.K. Ghoshal, M.K. Purkait, Preparation, characterization and performance studies of polysulfone membranes using PVP as an additive, J. Membr. Sci., 315 (2008) 36–47.
[20] H. Basri, A.F. Ismail, M. Aziz, Polyethersulfone (PES)-silver composite UF membrane: Effect of silver loading and PVP molecular weight on membrane morphology and antibacterial activity, Desalination, 273 (2011) 72–80.
[21] M.Z. Yunos, Z. Harun, H. Basri, A.F. Ismail, Studies on fouling by natural organic matter (NOM) on polysulfone membranes: Effect of polyethylene glycol (PEG), Desalination, 333 (2014) 36–44.
[22] Y. Ma, F. Shi, J. Ma, M. Wu, J. Zhang, C. Gao, Effect of PEG additive on the morphology and performance of polysulfone ultrafiltration membranes, Desalination, 272 (2010) 51–58.
[23] E.M. Van Wagner, A.C. Sagle, M.M. Sharma, Y.-H. La, B.D. Freeman, Surface modification of commercial polyamide desalination membranes using poly(ethylene glycol) diglycidyl ether to enhance membrane fouling resistance, J. Membr. Sci., 367 (2011) 273–287.
[24] T. Nguyen, F. Roddick, L. Fan, Biofouling of water treatment membranes: A review of the underlying causes, monitoring techniques and control measures, Membranes, 2 (2012) 804–840.
[25] S. Zanini, M. Muller, C. Riccardi, M. Orlandi, Polyethylene glycol grafting on polypropylene membranes for anti-fouling properties, Plasma Chem. Plasma Process., 27 (2007) 446–457.
[26] K. Abe, K. Higashi, K. Watabe, A. Kobayashi, W. Limwikrant, K. Yamamoto, K. Moribe, Effects of the PEG molecular weight of a PEG-lipid and cholesterol on PEG chain flexibility on liposome surfaces, Colloids Surf., A, 474 (2015) 63–70.
[27] J.M. Harris, Poly (ethylene glycol) chemistry: biotechnical and biomedical applications, Springer, 1992.
[28] A. Akbari, R. Yegani, B. Pourabbas, A. Behboudi, Fabrication and study of fouling characteristics of HDPE/PEG grafted silica nanoparticles composite membrane for filtration of Humic acid, Chem. Eng. Res. Des., 109 (2016) 282–296.
[29] Y. Liao, T.P. Farrell, G.R. Guillen, M. Li, J.A.T. Temple, X.-G. Li, E.M.V. Hoek, R.B. Kaner, Highly dispersible polypyrrole nanospheres for advanced nanocomposite ultrafiltration membranes, Mater. Horiz., 1 (2014) 58–64.
[30] S. Mondal, J.L. Hu, Microstructure and water vapor transport properties of functionalized carbon nanotube-reinforced dense-segmented polyurethane composite membranes, Polym. Eng. Sci., 48 (2008) 1718–1724.
[31] Y. Xie, C.A.S. Hill, Z. Xiao, H. Militz, C. Mai, Silane coupling agents used for natural fiber/polymer composites: A review, Composites, Part A, 41 (2010) 806–819.
[32] G. Cantero, A. Arbelaiz, R. Llano-Ponte, I. Mondragon, Effects of fibre treatment on wettability and mechanical behaviour of flax/polypropylene composites, Compos. Sci. Technol., 63 (2003) 1247–1254.
[33] M.A. Sibeko, A.S. Luyt, Preparation and characterization of vinylsilane crosslinked high-density polyethylene composites filled with nanoclays, Polym. Compos., 34 (2013) 1720–1727.
[34] M. Kazayawoko, J.J. Balatinecz, L.M. Matuana, Surface modification and adhesion mechanisms in woodfiber-polypropylene composites, J. Mater. Sci., 34 (1999) 6189–6199.
[35] A. Akbari, R. Yegani, B. Pourabbas, Synthesis of high dispersible hydrophilic poly (ethylene glycol)/vinyl silane grafted silica nanoparticles to fabricate protein repellent polyethylene nanocomposite, Eur. Polym. J., 81 (2016) 86–97.
[36] A. Akbari, R. Yegani, B. Pourabbas, Synthesis of poly (ethylene glycol) (PEG) grafted silica nanoparticles with a minimum adhesion of proteins via one-pot one-step method, Colloids Surf., A, 484 (2015) 206–215.
[37] J. Goldstein, Scanning Electron Microscopy and X-ray Microanalysis: Third Edition, Springer US, 2003.
[38] G. Bolton, D. LaCasse, R. Kuriyel, Combined models of membrane fouling: Development and application to microfiltration and ultrafiltration of biological fluids, J. Membr. Sci., 277 (2006) 75–84.
[39] H. Yan, S. Li, Y. Jia, X.Y. Ma, Hyperbranched polysiloxane grafted graphene for improved tribological performance of bismaleimide composites, RSC Advances, 5 (2015) 12578–12582.
[40] D.R. Lloyd, K.E. Kinzer, H.S. Tseng, Microporous membrane formation via thermally induced phase separation. I. Solid-liquid phase separation, J. Membr. Sci., 52 (1990) 239–261.
[41] Y. Jafarzadeh, R. Yegani, S.B. Tantekin-Ersolmaz, Effect of TiO_2 nanoparticles on structure and properties of high density polyethylene membranes prepared by thermally induced phase separation method, Polym. Adv. Technol., 26 (2015) 392–398.
[42] J. Duan, J. Gregory, Coagulation by hydrolysing metal salts, Adv. Colloid Interface Sci., 100–102 (2003) 475–502.
[43] J.-D. Lee, S.-H. Lee, M.-H. Jo, P.-K. Park, C.-H. Lee, J.-W. Kwak, Effect of coagulation conditions on membrane filtration characteristics in coagulation-microfiltration process for water treatment, Environ. Sci. Technol., 34 (2000) 3780–3788.